

Sensitivity Analysis of Unsteady Flow Fields and Numerical Experiments for Optimal Measurement

Takashi Misaka
Shigeru Obayashi

Institute of Fluid Science, Tohoku University
Sendai, 980-8577
Japan
misaka@edge.ifs.tohoku.ac.jp

Abstract

Difficulty of data assimilation arises from a large difference between the sizes of a state vector to be determined, i.e., the number of spatiotemporal grid points of a discretized numerical model, and a measurement vector, i.e., amount of measurement data. Flow variables on a large number of grid points are hardly defined by spatiotemporally limited amount of measurement data that poses an underdetermined problem. In this study we conduct sensitivity analysis of a vortex flow field by the use of an adjoint method. The idea of optimal/targeted observation in meteorology which aim to effectively determine a flow state by limited observations is interpreted in fluid dynamic problems where unsteady flows of much smaller scales are of interest.

Key words: sensitivity analysis, 4D-Var, large-eddy simulation.

Introduction

The use of observation data to improve a numerical prediction is known as data assimilation method in meteorological and oceanography communities [1]. The data assimilation is based on the optimal control theory. As a consequence there are two major approaches: sequential and variational methods, where the former includes a Kalman filter. The application of these methods to large scale problems in meteorology made the development of data assimilation methods slightly independent from optimal control studies, that is, the effort is put into the reduction of numerical costs of those methods. One example is the invention of ensemble Kalman filter, which approximately represents the system error covariance by an ensemble of model runs. By this the cost of matrix operations in Kalman filter can be drastically reduced. The numerical cost of variational methods such as the four-dimensional variational method (4D-Var) is usually smaller than the ensemble Kalman filter, therefore, the introduction of the 4D-Var into the operational weather forecast was earlier than that of ensemble Kalman filter. However, the cost for maintaining the adjoint code in the 4D-Var and the need for parallel computation accelerate the use of ensemble Kalman filters in meteorological community. Because of its rational approach to estimate a true state based on both measurement and simulation, the application of data assimilation methods is not limited to the area of meteorological and oceanographic studies.

We have been studying the applicability of data assimilation methods in aeronautical researches. Numerical simulations of atmospheric turbulences such as clear air turbulence and aircraft wake turbulence were performed with the 4D-Var method based on an aeronautical computational fluid dynamics (CFD) code [2,3]. Recent attempt is the mitigation of uncertainty of Reynolds-averaged Navier-Stokes (RANS) turbulence modeling by the use of ensemble Kalman filter, where parameters of the Spalart-Allmaras turbulence model are optimized based on pressure measurement around an airfoil [4]. On the other hand, a classical nudging technique is used to initialize aircraft wake in a computational domain to simulate realistic wake turbulence, where a high-fidelity RANS flow field is nudged instead of measurement data [5]. Nevertheless, the numerical approach used there is

very similar to that of data assimilation. Based on experiences gained from those applications our interest is to have a more general guidance to apply data assimilation methods successfully to problems with given conditions for measurement and simulation.

As a small step to that direction, the present study is an attempt to investigate the impact of measurement in a data assimilation system by a sensitivity analysis method and to use the information for optimal/targeted measurements. Here again we refer the preceding work of sensitivity analysis in meteorology [6]. We consider here an idealized situation in numerical experiments, i.e., a two vortex system where self-induced advection velocity realizes a transient flow field. The impact of the number of measurement points is firstly investigated, and the possibility of optimal measurement is exploited in the numerical experiments where locations of the measurement points are optimized to use the limited number of measurement points efficiently.

Approach

In this study we employ the 4D-Var method. The objective of data assimilation based on the 4D-Var method is to obtain an initial flow condition which reproduces corresponding measurements during a certain time period (assimilation window) [1]. Figure 1 shows a schematic of the 4D-Var method. Vertical and horizontal axes show flow state and time, respectively. A solid line shows a trajectory of a real flow state. Broken lines show trajectories of the simulated flow state starting from different initial conditions. The 4D-Var method is the method to obtain the initial condition of the real flow state by evaluating the difference of these trajectories within a assimilation window.

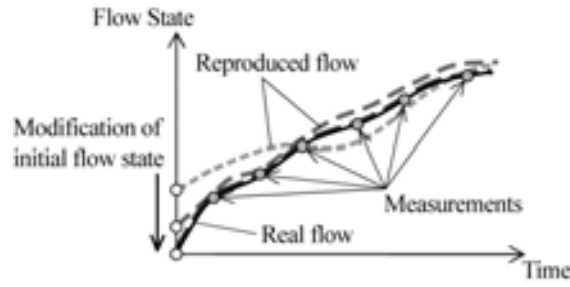


Figure 1. Schematic of data assimilation based on 4D-Var method.

The differences of measurements (usually measurements have less information compared to the numerical simulation) and corresponding numerical results evaluated by conducting the numerical simulation over a period of time are represented as an objective function with respect to an initial flow variable \mathbf{Q}_0 ,

$$J(\mathbf{Q}_0) = \frac{1}{2} \sum_{i=1}^N [H_i(\mathbf{Q}_i) - \mathbf{y}_i]^T \mathbf{R}_i^{-1} [H_i(\mathbf{Q}_i) - \mathbf{y}_i]. \quad (1)$$

Here, H_i is an observation operator which converts the dimension of computational flow variables into that of measurement data to evaluate these differences. Subscript i shows a time step of the flow computation and N is the total time number of the time steps. Equation (1) is a function of \mathbf{Q}_0 , that is, the data assimilation process is formulated as a minimization problem of $J(\mathbf{Q}_0)$ with control variables of \mathbf{Q}_0 . The 4D-Var method has a capability to treat measurement error through a measurement error covariance matrix \mathbf{R}_i , where its elements are the covariance between each measurement points. In this study \mathbf{R}_i is set to unit matrix. Basically the covariance matrix defines relative importance of measurements; therefore, we do not consider the effect in the present numerical experiments.

To obtain the gradient of $J(\mathbf{Q}_0)$ used for the minimization of $J(\mathbf{Q}_0)$, a Lagrange function is introduced using a Lagrange multiplier vector $\boldsymbol{\lambda}_i$. The procedure to obtain the gradient is finally written as follows [2]:

$$\boldsymbol{\lambda}_{N+1} = 0, \quad (2)$$

$$\boldsymbol{\lambda}_i = \mathbf{M}_i^T \boldsymbol{\lambda}_{i+1} + \mathbf{H}_i^T [H_i(\mathbf{Q}_i) - \mathbf{y}_i], \quad (i = N \sim 0), \quad (3)$$

$$\nabla J(\mathbf{Q}_0) = \boldsymbol{\lambda}_0. \quad (4)$$

Equations (2)-(4) show that the gradient of $J(\mathbf{Q}_0)$ is obtained by the inverse time integration of $\boldsymbol{\lambda}_i$ using the adjoint operator \mathbf{M}_i^T with a force term: $\mathbf{H}_i^T[\mathbf{H}_i(\mathbf{Q}_i) - \mathbf{y}_i]$. After obtaining the gradient, the minimization of $J(\mathbf{Q}_0)$ is conducted by the quasi-Newton method through modifying the initial flow variable \mathbf{Q}_0 . The Hessian matrix is approximated using the limited-memory Broyden-Fletcher-Goldfarb-Shanno (BFGS) method. In this method, memory requirements are reduced because the approximated Hessian matrix is not stored explicitly.

Here we investigate the impact of measurement data on a retrieved flow field within a framework of the data assimilation system based on the 4D-Var method. The sensitivity of the cost function with respect to the observation vector \mathbf{y}_i is represented as follows [6]:

$$\nabla_{\mathbf{y}_i} J(\mathbf{Q}_0) = \mathbf{H}_i \mathbf{M}_{0,i} [\nabla_{\mathbf{Q}_0 \mathbf{Q}_0}^2 J(\mathbf{Q}_0)]^{-1} \nabla J(\mathbf{Q}_0), \quad (5)$$

where $\nabla_{\mathbf{Q}_0 \mathbf{Q}_0}^2 J(\mathbf{Q}_0)$ represents a Hessian matrix, and we can use the approximated Hessian matrix obtained from the limited-memory BFGS. A mapping of the sensitivity on measurement points onto the grid points of numerical simulation is performed as follows:

$$\mathbf{H}_i^T \nabla_{\mathbf{y}_i} J(\mathbf{Q}_0) = \mathbf{M}_{0,i} [\nabla_{\mathbf{Q}_0 \mathbf{Q}_0}^2 J(\mathbf{Q}_0)]^{-1} \nabla J(\mathbf{Q}_0). \quad (6)$$

For flow simulations we employ incompressible Navier-Stokes equations. The equations are discretized by the fully-conservative fourth-order central difference scheme [7]. Time integration is performed by third-order low storage Runge-Kutta scheme [8]. The Lagrangian dynamic model is used as a subgrid scale model for large-eddy simulation [9], which has superiority in vortical flows [10]. The adjoint codes are derived first by linearizing the above equations, then by rewriting it from backward by replacing inputs and outputs of each code line. The latter operation corresponds to a transpose of the matrix composed of coefficients of the linearized Navier-Stokes equations. The both Navier-Stokes and the adjoint codes are parallelized by using message passing interface (MPI) for large scale computations.

The development of linear and adjoint codes can be done step by step processes in the following way. First the derived linear code is checked by $|M(\mathbf{Q} + \alpha\delta\mathbf{Q}) - M(\mathbf{Q})|/|\alpha\mathbf{M}\delta\mathbf{Q}| - 1 = O(\alpha)$ where the left-hand-side decreases with the order of α . It is also possible to check the angle: $[M(\mathbf{Q} + \alpha\delta\mathbf{Q}) - M(\mathbf{Q})]^T [\mathbf{M}\delta\mathbf{Q}] / (|M(\mathbf{Q} + \alpha\delta\mathbf{Q}) - M(\mathbf{Q})| |\mathbf{M}\delta\mathbf{Q}|) - 1 = O(\alpha^2)$, which decreases with α^2 . The adjoint code is a transpose of the linearized code and is derived line by line without composing an explicit matrix. In the adjoint code, the following relation $[\mathbf{M}\mathbf{Q}]^T \mathbf{M}\mathbf{Q} - \mathbf{Q}^T [\mathbf{M}^T [\mathbf{M}\mathbf{Q}]] = O(\epsilon)$ is true on the order of 10^{-14} in the Fortran double precision real. The above processes can be conducted in small program modules such as convective and diffusion terms of Navier-Stokes equations as well as a whole code including all terms and a time integration part. Finally, the computed gradient is confirmed by $|J(\mathbf{Q} + \alpha\delta\mathbf{Q}) - J(\mathbf{Q})|/[\alpha\delta\mathbf{Q}^T (\nabla J(\mathbf{Q}))] - 1 = O(\alpha)$, where again the left-hand-side decreases with α . Table 1 shows the computed gradient, while Table 2 shows the strong scaling of the gradient computation in parallel where the number of total grid points is fixed with increasing processor numbers.

Table 1. Confirmation of gradient computation.

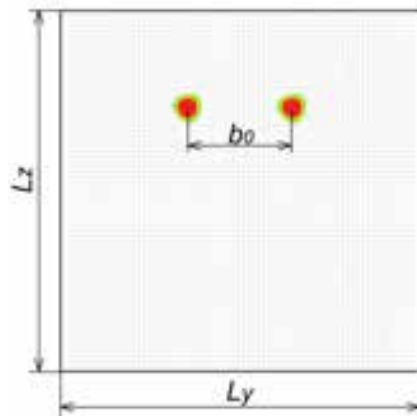
α	$\nabla J(\mathbf{Q}_0)$
1.E+1	1.394683E+1
1.E+0	1.614762E+0
1.E-1	1.626424E-1
1.E-2	1.626592E-2
1.E-3	1.626596E-3
1.E-4	1.626548E-4
1.E-5	1.623851E-5
1.E-6	1.414659E-6
1.E-7	-2.144048E-6

Table 2. Strong scaling of the gradient computation.

Number of processors	Wall-clock time [sec]
8	1476.56
16	638.72
32	277.10
64	184.39
128	93.93
256	109.62
512	42.15

The computational setting is as follows (see also Fig. 2). We consider a flow field defined by a pair of Lamb-Oseen vortices which are characterized by vortex circulation $\Gamma_0 = 300 \text{ m}^2/\text{s}$, vortex core radius of $r_c = 4 \text{ m}$ and vortex separation $b_0 = 40 \text{ m}$. The vortex flow field is initialized two-dimensionally along x -axis within a domain bounded by $L_x = 64 \text{ m}$, $L_y = 128 \text{ m}$, $L_z = 128 \text{ m}$ sides. A constant mesh spacing of 2 m is used for all three spatial directions. Time integration is conducted until one tenth of vortex reference time t_0 , i.e., 3.3 s in the present condition, where the vortex pair moves a distance of one tenth of vortex separation b_0 during this period. Parallel computation is performed by a domain decomposition approach, where typically $n_x = 2$, $n_y = 4$, $n_z = 4$ processors are used in the present study.

Numerical experiment is conducted first by generating reference flow fields starting from the above conditions. In this process we acquire pseudo measurement data based on the following strategies, i.e., velocity components of the all grid points are considered as measurements (Case 1), velocity components from every second grid points in both y - and z -directions are used (Case 2), and the data on every fourth grid points are used as measurements (Case 3). Compared to Case 1, the number of measurements is one fourth in Case 2 and one sixteenth in Case 3. Then the 4D-Var cycle (forward time integration for the evaluation of a cost function, backward time integration of the adjoint code, Hessian matrix computation with limited-memory BFGS and linear search) is started with an arbitrary flow field, where we consider a weaker vortex pair compared to the reference flow field ($\Gamma_0 = 200 \text{ m}^2/\text{s}$, $r_c = 6 \text{ m}$ and $b_0 = 60 \text{ m}$). Adaptive measurement processes starts after a few iterations of the 4D-Var cycle. Having an approximated Hessian matrix and the gradient from the adjoint code, the observation sensitivity can be computed by using Eq. (5). In this paper we only consider the observation sensitivity at the beginning of time integration. Using the observation sensitivity mapped onto the numerical grid, measurement points are redistributed based on the magnitude of the observation sensitivity, where the total number of the measurement points is kept constant.

**Figure 2. Computational domain with grid lines and initial vortex positions.**

Results

Figure 3 shows histories of cost function defined by Eq. (1) for three measurement strategies, while the global error is evaluated by using the whole mesh points. This indicates that the decrease of the cost function in the 4D-Var is not always connected with the convergence of the retrieved flow field to the reference flow field. In Case 1 the value of the cost function and the global error are identical because three velocity components on all grid

points in the domain are used as measurements. The value of the cost function is proportional to the number of measurement points and time steps, therefore, the values reduce from Case 1 to Case 3. On the other hand, the decrease of the global error becomes slow as the number of measurements is reduced. This confirms that there is a limitation for defining a flow field by using a limit number of measurements, i.e., a number smaller than a degree of freedom in the numerical model. Please note that the behaviors of the cost function and the global error might vary depending on the data assimilation methods used and parameters included in the optimization algorithms, however, the tendency shown here may be true also for other methods.

Figure 4 shows a similar plot as Fig. 3 but with optimal measurement strategies described above. Here the redistribution of measurement points is done in the every 5th iteration of the 4D-Var assimilation cycle. Until 5th iteration the values of cost function and the global error are the same as those of Fig. 3. At the 6th iteration the value of cost function rapidly increases because the measurement points are redistributed to the regions where the global error is relatively large. The cost function again decreases after a few iterations. During the reduction of cost function, the global error values are also decreased in Case 2 and Case 3, and the values become smaller than those in Fig. 3. This implies that the global error can be effectively reduced by locating measurement points on places where the relative error is large. And it becomes possible by checking the observation sensitivity in the data assimilation cycle. Even with the adaptive measurement strategy the global error is larger than the Case 1 where measurements of all grid points are given.

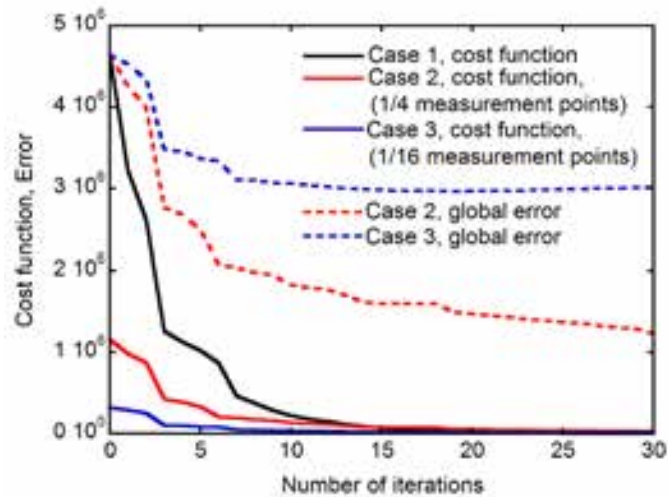


Figure 3. Histories of cost function and global error with different measurement points

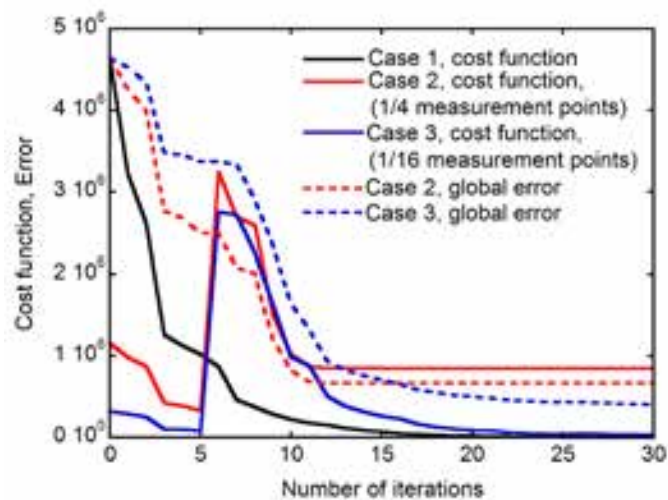


Figure 4. Histories of cost function and global error with adaptive measurement

Figure 5 shows the distribution of measurement points in Case 2, where every second grid points in both y - and z -directions have measurements. The total number of measurement points is one fourth of that in Case 1. Figure 5(a) shows the initial distribution, and Fig. 5(b) shows the distribution after the first rearrangement of measurement points. These measurement points are colored by the magnitude of observation sensitivity at those locations. Since the measurement points are redistributed using the grid points of the numerical simulation, the measurement points do not come closer than the grid spacing. The resolution of measurements finer than that of numerical simulation may not improve the retrieved flow field in the context of data assimilation. Figure 5(c) shows the distribution of measurement points at 16th iteration, where the distribution is similar to that of Fig. 5(b) where the points are clustered near vortices. In the same way Fig. 6 show the Case 3 where every fourth grid points in both y - and z -directions has measurements. The total number of measurements is one sixteenth of that in Case 1. As in the Case 2 the measurement points are clustered near vortices at the first adaptation.

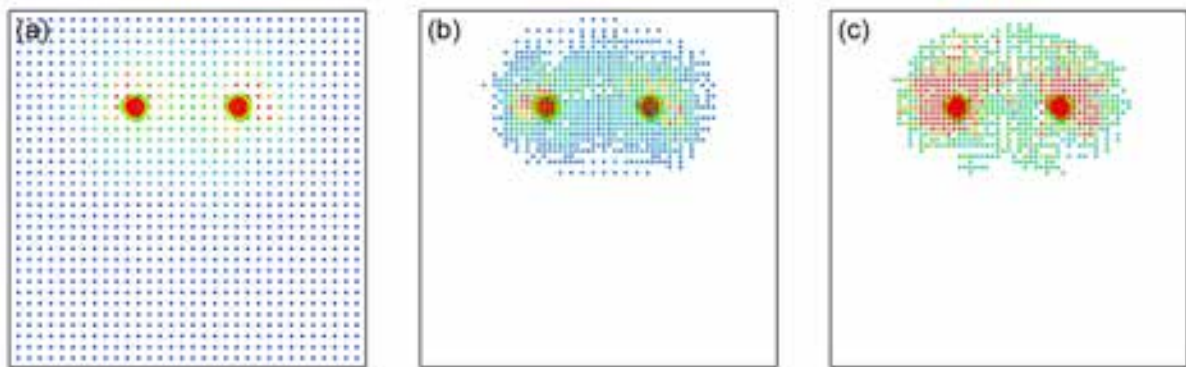


Figure 5. Distribution of measurement points with optimal measurement (Case 2), where the color of the points shows the magnitude of observation sensitivity at those locations.

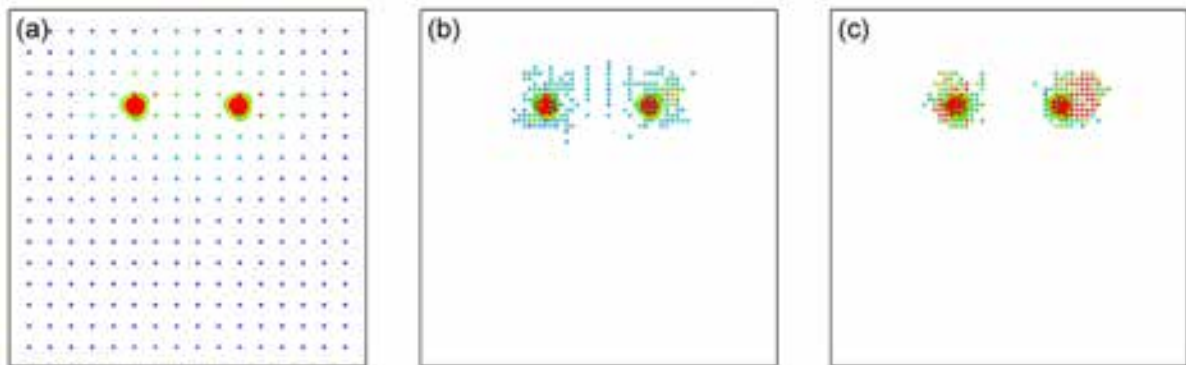


Figure 6. Distribution of measurement points with optimal measurement (Case 3), where the color of the points shows the magnitude of observation sensitivity at those locations.

Conclusions

In this study we conduct sensitivity analysis of a vortical flow field by the use of an adjoint method. The idea of optimal/targeted observation in meteorology which aim to effectively determine a flow state by limited observations are interpreted in fluid dynamic problems where unsteady flows of much smaller scales are of interest. The present approach enables to investigate the impact of measurements in an actual data assimilation system of the 4D-Var. We investigated a simple case with a pair of vortices which move due to self-induced advection velocity. The amount of measurement points affects the convergence of the cost function as well as the global error against the reference flow field. The optimal measurement strategy based on the observation sensitivity effectively redistributes measurement points near vortices. This results in the further reduction of the global error. As for future work the impact of the number of measurements in time as well as of assimilation window size should be investigated. A series of investigations might show the applicability limit of the 4D-Var for given experimental and numerical conditions.

Acknowledgements

Authors would like to thank the Advanced Fluid Information Research Center at Institute of Fluid Science, Tohoku University for computational resources used in this study.

References

- [1] E. Kalnay, *Atmospheric Modeling, Data Assimilation and Predictability*, Cambridge University Press, 2003.
- [2] T. Misaka, S. Obayashi, and E. Endo, "Measurement-Integrated Simulation of Clear Air Turbulence Using Four-Dimensional Variational Method," *Journal of Aircraft*, Vol. 45, pp. 1217-1229, 2008.
- [3] T. Misaka, S. Obayashi, I. Yamada, and Y. Okuno, "Assimilation Experiment of Lidar Measurements for Wake Turbulence," *JSME Journal of Fluid Science and Technology*, Vol. 3, pp. 512-518, 2008.
- [4] H. Kato, S. Obayashi, "Statistical Approach for Determining Parameters of a Turbulence Model," *IEEE 15th International Conference on Information Fusion (FUSION)*, pp. 2452-2457, July 2012.
- [5] T. Misaka, F. Holzäpfel, T. Gerz, "Wake Evolution of Wing-Body Configuration from Roll-Up to Vortex Decay," *50th AIAA Aerospace Science Meeting*, AIAA Paper 2012-0428, January 2012.
- [6] D. N. Daescu, "On the Sensitivity Equations of Four-Dimensional Variational (4D-Var) Data Assimilation," *Monthly Weather Review*, Vol. 136, pp. 3050-3065, 2008.
- [7] Y. Morinishi, T. S. Lund, O. V. Vasilyev, and P. Moin, "Fully Conservative Higher Order Finite Difference Schemes for Incompressible Flow," *Journal of Computational Physics*, Vol. 143, pp. 90-124, 1998.
- [8] J. H. Williamson, "Low-Storage Runge-Kutta Schemes," *Journal of Computational Physics*, Vol. 35, pp. 48-56, 1980.
- [9] C. Meneveau, T. S. Lund, and W. H. Cabot, "A Lagrangian Dynamic Subgrid-Scale Model of Turbulence," *Journal of Fluid Mechanics*, Vol. 319, pp. 353-385, 1996.
- [10] T. Misaka, F. Holzäpfel, I. Hennemann, T. Gerz, M. Manhart, and F. Schwertfirm, "Vortex Bursting and Tracer Transport of a Counter-Rotating Vortex Pair," *Physics of Fluids*, Vol. 24, pp. (025104-1)-(025104-21), 2012.